Data analysis methods for neuroimaging data pre-processing to decode cognitive tasks using logistic regression for BCI applications

Francis Mason[1] Student Member, *IEEE*, Sujit Roy[2] and Girijesh Prasad[1] Senior Member, *IEEE*

***Abstract*—Brain-Computer Interfaces permit neural activity to be directly interpreted and used for applications, like therapeutic replacement of lost function (e.g. stroke) or to supplement existing function (e.g. handsfree applications). Two major challenges for BCI are accurate interpretation of neural activity and signal processing speed for real-time applications i.e. correctly decode a user's intent and the timely execution of that intent. Magnetoencephalography has advantages over Electroencephalography with respect to spatial and temporal resolution which could potentially allow better decoding of brain activity. High spatial and temporal resolution using MEG generates a large volume of data which must be rapidly preprocessed and classified correctly for practical real-time BCI. This paper presents a simple data processing technique to clean, normalise and reduce data dimensionality, for optimal class label decoding using a simple Logistic Regression classifier. Good decoding performance was achieved using an off-line MEG dataset, with or without data dimensionality reduction, comparable to more complex data pre-processing methods and classifiers already studied.**

I. INTRODUCTION

Brain-Computer Interfaces (BCI) can be defined as a communication system that does not depend on the normal brain output pathways of peripheral nerves and muscles [9]. It is an independent method for understanding brain activity so a user's intention can be used to communicate directly with an external device. BCI has the potential to supplement, assist or repair human sensory-motor function with a clear application in aiding recovery through neural feedback of people with neuromuscular diseases. BCI has four main components: (1) Signal acquisition (2) Feature extraction and identification, (3) Feature classification of a desired intent, and (4) Output device to action an intent, with neural feedback. Signal processing must occur ≤0.2 seconds for practical application so a noticeable delay between an intent and a response is not introduced [3,4,5,9,12,13].

Measuring sensorimotor rhythms (SMR) during imagery is gaining favour for real time BCI. This frequency and/or amplitude change in response to a task include the mu rhythm (8–12Hz) from the sensory cortex with a beta rhythm component (18–26Hz) from the motor area, hence the term "Sensorimotor". It is broadly accepted that motor imagery (MI) involves the same brain regions and functions which are involved in motor execution (ME) [3,13,15,22]. It is possible for a person to be trained to modulate the mu and/or beta rhythms and thus use MI for BCI control. For example, BCI-Electroencephalography (EEG) with MI was successfully used for paralysed limb rehabilitation using mu and beta band rhythm control [16].

EEG is frequently deployed for real time BCI due to its excellent temporal resolution and ease of use [26-28]. Magnetoencephalography (MEG) is closely related to EEG but has the advantage of being less prone to data distortion, so providing more precise signal location. MEG uses superconducting sensors and the principle of magnetic induction to detect and capture electrical brain signals using two types of sensors, gradiometers and magnetometers, the former having better signal to noise suppression [4,5]. It generates a large quantity of multi-dimensional data which requires a lot of processing power to interpret, limiting its use for real time BCI. However, the evolution in computing power and Machine Learning techniques allow faster, more accurate signal processing, thus potentially allowing MEG to be used for real-time BCI [5,7,9-16]. Real-time studies using MEG-BCI are more limited than for EEG, but results mirror those obtained for EEG-BCI, showing that MEG can measure mu and beta SMR rhythms during MI with good classifier accuracy achieved. Principle Component Analysis (PCA) with a simple signal spatial filtering method exhibited good real-time MEG-BCI control using mu rhythm which was comparable to EEG-BCI [24]. Logistic Regression (LR), k-Nearest Neighbors (kNN), Linear Discriminant Analysis (LDA), Gaussian Naïve Bayes (GNB) and Support Vector Machine (SVM) have shown accuracies ranging from 50-90% depending on the classifier type, the number of features used and if it was trained and tested with intra-session (same dataset) or inter-session data (different dataset) [7,10,11]. SVM and kNN demonstrated more stable performance compared to LDA, which had reduced accuracy with a higher number of channels, when trained with <300 features [11]. Like EEG, MEG based classifier accuracy can be sustained or improved with reduced channels [3,10,11].

The study objective is to develop a basic signal pre-processing technique using off-line MEG data, that gives good classification accuracy with the simplest classifier and the minimum amount of data. This methodology could then be later tested using real-time MEG-BCI where signal processing time is essential and thus simplicity is beneficial.

II. METHODOLOGY

A. Experimental protocol

MEG datasets were acquired from 17 healthy volunteers who consented to take part in the study. Demographic details

Funding support from The Department of Science and Technology (DST), India and UK India Education and Research Initiative (UKIERI) Thematic Partnership project (DST-UKIERI-2016-17-0128), Invest Northern Ireland (InvestNI) and The University of Ulster, Northern Ireland Functional Brain Mapping Facility (NIFBM) project (1303/101154803).

[1]Intelligent Systems Research Centre (ISRC), School of Computing, Engineering and Intelligent Systems, The University of Ulster, Londonderry, UK, [2]The University of Manchester, Manchester, UK, M15 6PB. Corresponding author: Francis Mason: francisgmason1@gmail.com

of participants have been previously reported [25]. This study used data from 13 of the 17 healthy individuals; 11 male and 2 females, with a mean age of 29.2 (±5.9) years. Data was recorded using an Elekta Neuromag Triux MEG scanner with 204 gradiometer and 102 magnetometers. Volunteers sat 80cm from a screen where 4 imagery tasks were displayed, including imagined limb movement, calculation and language. The magnetic field density changes to each stimulus were recorded at 1000Hz across the full 0.1-330Hz bandwidth. Fig. 1 shows the experimental protocol used.

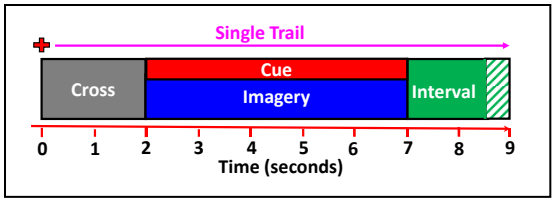

Figure 1. Experimental protocol used for each MEG trial.

Upon appearance of a screen cue, each task was performed i.e. movement of both hands, movement of both feet, subtraction of numbers or generation of an English word beginning with the letter displayed. Each session involved 50 trials for each task so a total of 200 trials were performed by each candidate during each session. Each trial started with a rest period of 2 seconds followed by 5 seconds for the imagery task, with the cue visible. A random interval (ITI) between trials of 1.5 to 2 seconds was used [4,25].

B. Data Pre-processing

All data handling and analysis herein, used Python v3.7.3. The MNE-Python open-source module for processing and analysis of neuroimaging data were applied [6,8].

Identification of bad channels and signal filtering: visual inspection of channels for flatlining, excessive noise or sensor malfunction, as well as frequency analysis were used to select bad channels across the full 0.1-330Hz bandwidth. Bad channels were removed and interpolated based on signals from adjacent sensors to maintain data dimensionality for classifier training and testing. The trigger channel (STI101) encoded the events during the experimental recordings and was used for raw data event identification. Only data from the 204 gradiometers were used at 1000Hz sampling frequency [4,5]. The signals were band filtered (firwin zero-phase Finite Impulse Response or FIR filter) at different frequency ranges: delta (δ: 1-4.5Hz), theta (θ: 4.5-8.5Hz), alpha (α: 8.5-11.5Hz), low beta (β: 11.5-15.5Hz), beta (β: 15.5-22Hz), high beta (β: 22-30Hz), low gamma (γ: 30-49Hz) and high gamma (γ: 51-99Hz). The delta frequency high-pass filter was set at 1.0 Hz to attenuate interference due to biological noise (e.g. breathing) and magnetic noise. Notch filtering was applied to attenuate electrical interference (50Hz, 100Hz) and the 49-51Hz frequency band was ignored.

Epoched, evoked and grand averaged data: the cleaned data were epoched to detect actual deflections related to a response. A maximum gradiometer reading rejection limit of $4000e^{-13}$ was set based on literature review [6,8]. A time for epoch creation from 0 to 4 seconds after applying the stimulus was used without a baseline period. The evoked response was calculated by averaging across epochs to remove interference and to obtain a clearer overall signal response. The grand average was determined for all participants for each stimulus. The resulting signal response was visualised as Global Field Power (GFP), which is an unbiased measure of field strength at the scalp [17]. GFP is calculated as the Root Mean Square (RMS) for all sensor values at a given instant (Equation 1). It measures the standard deviation of the magnetic field strength for all sensors and shows how the average magnetic field strength (signal energy) varies at a given time instant but provides no information on the field distribution across the sensors [17]. RMS could also be applied to each sensor along the time dimension to provide an average power value per sensor for a time period under study. For this study, RMS was used to transform each raw sensor data into a power value per sensor before classifier training and testing. Table I illustrates how the normality of the grand averaged data improved by applying the RMS transform. Kurtosis and skewness values confirm the transformation of a highly right (positively) skewed and peaked (leptokurtic) distribution to a more Gaussian distribution for better classifier performance.

TABLE I. SKEWNESS & KURTOSIS OF AMPLITUDE SQUARED & ROOT MEAN SQUARED DENSITY DISTRUBUTION BY STIMULUS.

Stimulus	Amplitude Squared		RMS Amplitude	
	Skewness	*Kurtosis*	*Skewness*	*Kurtosis*
HAND	1.80	4.55	0.25	-0.10
FOOT	2.67	9.14	0.34	0.11
WORD	1.96	5.67	0.39	0.19
MATH	2.30	5.73	0.64	0.66

It has been reported [18] that the geometric mean is better than the arithmetic mean for averaging frequency response spectra, minimising bias due to noise, nonlinearity and outliers. It is calculated as the product of a series of numbers raised to the reciprocal of the number of values (Equation 2). Equations 1 and 2 were combined to give a geometric RMS calculation (Equation 3) which was applied to the raw MEG data for each sensor along the time dimension.

$$RMS = \sqrt{\frac{x_1^2 + x_2^2 + x_1^2 + \ldots . x_n^2}{n}} = \sqrt{Arithmetic\ Mean\ of\ Power} \quad (1)$$

$$Geometric\ Mean = \sqrt[\frac{1}{n}]{x_1 * x_2 * x_3 * \ldots x_n} \quad (2)$$

$$Geometric\ RMS = \sqrt{Geometric\ Mean\ of\ Power} \quad (3)$$

C. Classifier evaluation and optimisation.

Supervised classification methods, LR, SVM, LDA, GNB, kNN and RF were evaluated [1]. The ability to distinguish between the binary class labels was compared: Hand-Foot (H-F), Hand-Word (H-W), Hand-Calculation (H-C), Foot-Word (F-W), Foot-Calculation (F-C) and Word-Calculation (W-C). 10-fold Cross Validation, repeated 5 times with shuffling, was applied for all classifier training using 100% of the session#1 data sets (Intra-session), and then tested with the session#2 data set (Inter-session). The classifier with the best inter-session, intra-session (cross validation score) and training accuracy was selected. Data scaling with the sklearn 'StandardScaler' was applied prior to

classification which standardises features by removing the mean and scaling to the data variance. The same scaling parameters were used for training and testing. Another sklearn package, was used for classifier hyper-parameter tuning 'GridSearchCV', which searches all combinations of specified parameters to determine an optimum combination.

It is highly desirable to reduce the number of features needed by a classifier in order to minimise processing time without loss of classifier accuracy. Two feature selection methods were evaluated: RFECV and ELI5. RFECV is a wrapper type feature selection method which uses a specified algorithm (SVM linear used) with 10-fold cross validation to measure feature importance. Predictions of the target variable are ranked and irrelevant features eliminated on each iteration. The weakest features are removed until the optimum number are obtained [20]. ELI5 evaluates feature importance by measuring how the accuracy score decreases when a feature is moved. Feature order is shuffled to introduce "noise" into the dataset while maintaining dimensionality to avoid classifier re-training [21].

III. Results

A. Global field power of grand averaged data

Figs. 2-5 show the GFP for the grand average evoked data by stimulus for delta, theta, alpha and low beta band filtered data. These bands had the highest signal response.

GFP peaks for all stimuli and all frequency bands in <0.25 seconds, returning to baseline in <1.0 second. Theta and alpha bands return to baseline in ≤0.5 seconds while low and high beta bands peak sooner and return to baseline quicker. Peak GFP reduces as frequency increases. The strong delta rhythm response is consistent with studies [19] on MI tasks without ME which display a delta band increase after 0.1 to 0.3 seconds after a stimulus and a further response after 0.35 to 0.55 seconds. The latter response is only observed for an MI task, suggesting a role in motor inhibition. It has been suggested that delta waves during MI suppress neural activity unrelated to task execution [19]. Theta wave occurrence is expected during task execution, as it's linked to working memory, information retrieval and focus [9,19]. Alpha rhythm is also expected as it is related to attention and inhibitory control for mental co-ordination of response [9,23]. Beta rhythms occur when alert and attentive, such as during problem solving, decision making and focused mental tasks. Low beta happens during captive thought and high beta during complex thought. The absence of a response in the gamma range is not surprising as it's linked to higher cognitive functions [9,19].

B. Alpha and low-beta frequency band analysis

This study focused on using the alpha and low beta frequency bands (8.5 to 15.5Hz) since this frequency band provided highest classifier accuracy (Fig.11).

The frequency band selected includes the mu rhythm (8-12Hz) which occurs in the sensorimotor brain region during ME or MI tasks. It is suppressed and replaced with beta waves during a task and restored after a task completes [22].

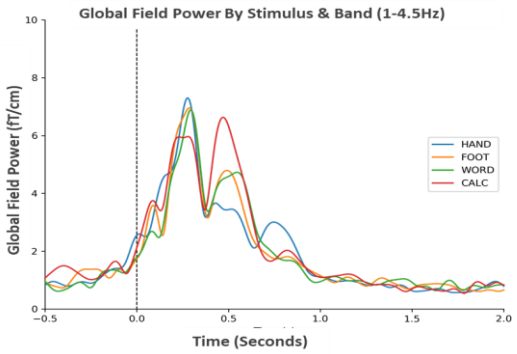

Figure 2. GFP by stimulus for delta 1-4.5Hz band filtered data.

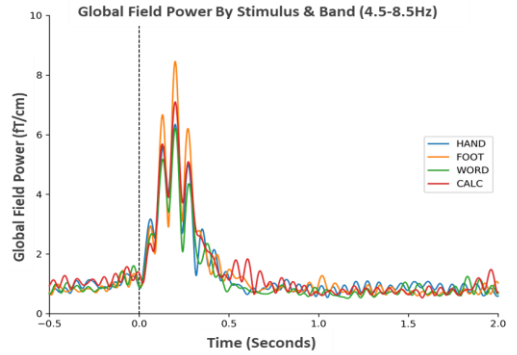

Figure 3. GFP by stimulus for theta 4.5-8.5Hz band filtered data.

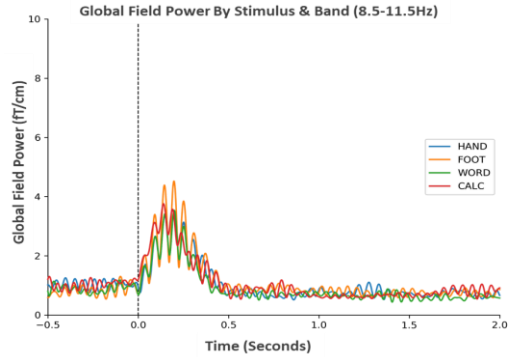

Figure 4. GFP by stimulus for alpha 8.5-11.5Hz band filtered data.

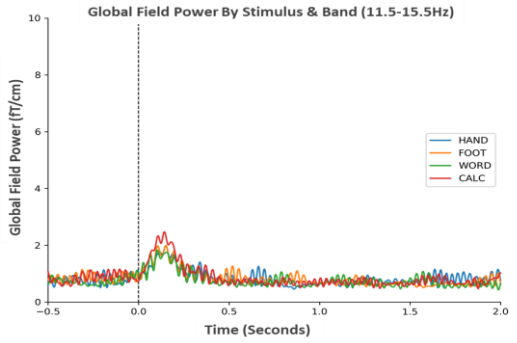

Figure 5. GFP by stimulus for low-beta 11.5-15.5Hz band filtered data.

This increase (ERS) or decrease (ERD) in response to MI causes inhibition and activation of specific brain regions. ERD activates regions involved in performing a task, while ERS inhibits regions irrelevant to it [22]. Delta, theta and gamma frequencies only exhibit ERS during a task suggesting that they are involved in neural inhibition processes and are thus not task specific [9,23].

The grand average evoked signal response in the 8.5-15.5Hz band frequency completes in <0.5 seconds from applying a stimulus. Figs. 6-9 are butterfly plots showing 1.5 seconds of magnetic field variation by sensor location (in colour) using grand averaged data for each stimulus in the alpha and low-beta bands. Each plot also shows scalp topographies at different times. Fig. 6 shows the response for the hand stimulus, which lasts 0.4 seconds with an ERD at 0.1 second, as expected for an MI task. Figs. 7-9 show the foot, word and calculation stimuli signal response which follow a similar pattern as the hand stimulus. The purple colouration show an apparent activation of the parieto-occipital sensory association cortex consistent with the somatosensory association area and alpha rhythm occurrence. A deeper purple colour for the hand stimulus suggests both hemispheres activity, while the lighter purple colour for foot, word and calculation stimuli, suggest more right hemisphere activity. Green colouration for word and calculation stimuli, suggest possible frontal lobe activation for higher mental functions (e.g. problem solving).

C. Classifier accuracy by frequency and class label

The LR classifier was selected for optimisation as it is the simplest and had the best overall performance (visually).

Fig.10 shows the performance of all classifiers for inter-session classification. Hypothesis testing using ANOVA (Pairwise Tukey HSD) and 95% confidence interval showed no statistical difference in the mean accuracy of the classification methods. However, LR and SVM (with linear kernel) were visually selected as classification accuracy was higher, ranging from 62-78% depending on the class label.

Fig.11 displays the average LR and SVM inter-session classification accuracy by frequency band using all channels. This confirms that alpha and low beta band filtered data give the highest inter-session classifier accuracy (LR alpha 70.5±5.3%%, LR low-beta 69.6±6.3%). The accuracy of the delta and theta band filtered data, although inferior (~64%), are less variable (±3%) than higher frequency bands (8.5-30Hz). The low variability may indicate a repeatable neural inhibition process during a task, as already reported [9,23].

D. LR classifier feature selection

The LR classifier could identify between class labels using >48 channels which were predominantly located on the occipital and parietal brain regions.

Fig. 12 shows the LR accuracy for inter-session and training data classification in 10 channel increments from 10 to 190 channels, using ELI5 and RFECV feature selection methods. ELI5 was a better feature selection method, needing less channels (~50) to reach optimum accuracy compared to RFECV (~100). ELI5 was selected for LR classifier training using ~204, ~100, ~50 and ~25 channels.

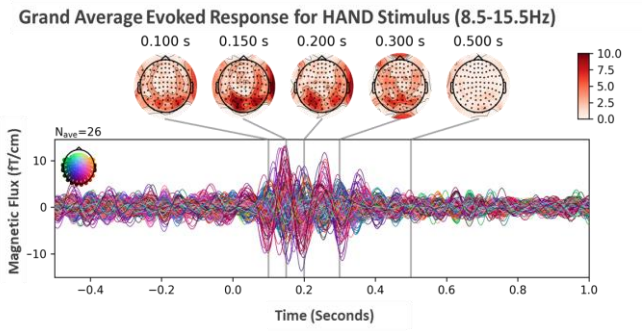

Figure 6. Grand average evoked response for hand stimulus (8.5-15.5Hz). Red, green and blue colours indicate sensor position (top left).

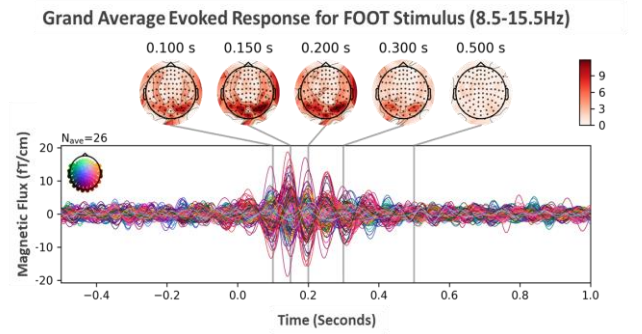

Figure 7. Grand average evoked response for foot stimulus (8.5-15.5Hz). Red, green and blue colours indicate sensor position (top left).

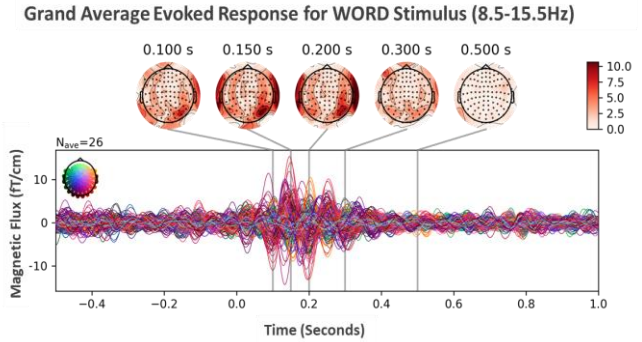

Figure 8. Grand average evoked response for word stimulus (8.5-15.5Hz). Red, green and blue colours indicate sensor position (top left).

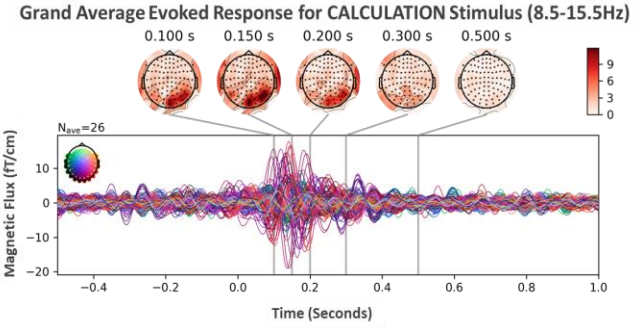

Figure 9. Grand average evoked response for calculation stimulus (8.5-15.5Hz). Red, green and blue colours indicate sensor position (top left).

Fig. 13 shows the top 21 to 30 channels for classification of each class label. Generally, the occipital and/or parietal brain regions are active for all class labels. The right temporal region is active, particularly for H-C, but also other class labels except H-F. There is some left temporal region activity for all class labels. H-W shows the most frontal lobe activity. These observations are consistent with dominant neural activity in the parietal and occipital lobes where the visual and somatosensory sensory cortexes are located. These brain regions are involved in processing visual sensory input and interpreting it to control MI or ME outputs.

E. Optimised LR classifier performance metrics

Table II shows the performance of the LR classifier with optimised hyper-parameters (kernel: liblinear, C: 0.1, Penalty: l2, multiclass: 'ovr') and different channel numbers (NoC). The classifier performed best with all sensor channels validating the proposed data pre-processing methodology. The intra- and inter-session accuracy was sustained with ≥99 channels. An exception was the H-F and W-C inter-session accuracies which improved slightly with 48 channels. H-W had the highest accuracy while H-F MI had the lowest for all scenarios. Accuracy was worse for inter-session classification as expected, due to varying conditions between experimental sessions (e.g. alertness, motivation and sensor position).

LR is better at "True Positive" prediction. Table II shows Area Under Curve (AUC), precision and recall metrics for the trained LR classifier. AUC measures how good a classifier is at discriminating the positive class while high precision means a low false positive rate and recall shows a classifiers ability to label all positive results correctly. AUC and precision for the inter-session LR classification exceed accuracy and recall. AUC is between 7% to 14% higher than accuracy depending on the class label. Unlike accuracy, AUC appeared to be more stable as channel numbers were reduced which was also reported previously for LDA [11].

TABLE II. LR CLASSIFIER METRICS BY AVG. CHANNEL NUMBER

AVG.	H-F	H-W	H-C	F-W	F-C	W-C	NoC
Intra-session Accuracy	69%	**83%**	**78%**	**83%**	**78%**	77%	204
	70%	82%	78%	81%	**78%**	**79%**	99
	69%	82%	73%	78%	76%	76%	48
	69%	79%	71%	76%	71%	73%	27
Inter-session Accuracy	62%	**78%**	**74%**	**75%**	**73%**	68%	204
	65%	77%	73%	74%	72%	**70%**	99
	65%	75%	71%	71%	68%	**70%**	48
	64%	71%	68%	68%	66%	68%	27
Inter-session AUC	73%	**89%**	**81%**	**83%**	**82%**	**82%**	204
	74%	88%	**81%**	82%	**82%**	**82%**	99
	73%	88%	**81%**	82%	78%	80%	48
	73%	85%	79%	80%	76%	79%	27
Inter-session Precision	66%	**81%**	**75%**	**79%**	**76%**	73%	204
	68%	80%	74%	78%	75%	73%	99
	69%	79%	**75%**	76%	71%	**74%**	48
	68%	76%	71%	72%	68%	73%	27
Inter-session Recall	62%	**78%**	**74%**	**75%**	**73%**	68%	204
	65%	77%	73%	74%	72%	**70%**	99
	65%	75%	71%	71%	68%	**70%**	48
	64%	71%	68%	68%	66%	68%	27

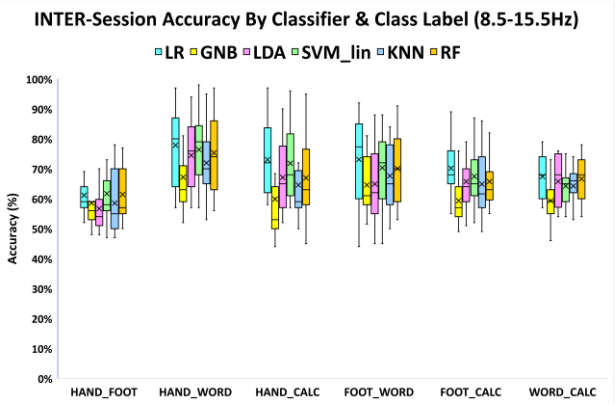

Figure 10. Inter-session classifier accuracy by type and class label.

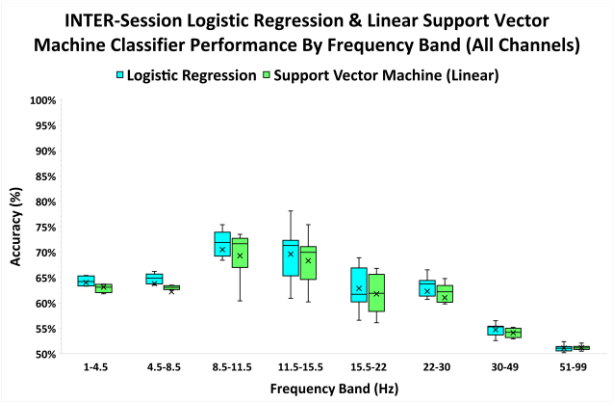

Figure 11. LR and SVM inter-session classifier accuracy by band.

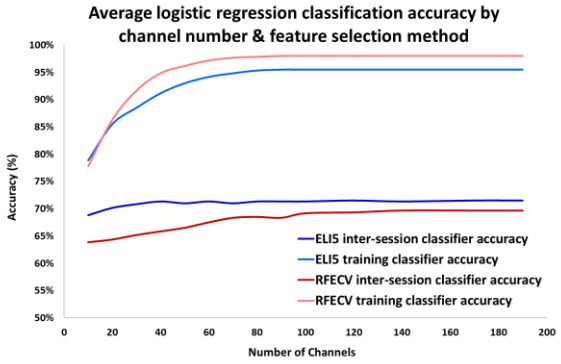

Figure 12. LR accuracy by channels and feature selection method.

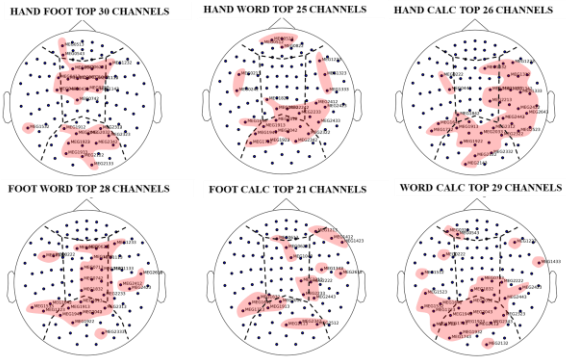

Figure 13. Top sensors from ELI5 feature selection by binary class label. Dotted line: frontal, left & right temporal, occipital and pareital regions.

F. *Summary of results*

The evoked response to stimuli and best sensor locations for binary class label classification, shows the importance of the occipital and parietal brain regions for task identification in the 8.5-15.5Hz frequency band. These brain areas are involved in visual and sensory processing, while alpha rhythm co-ordinates sensory response and low beta rhythm occurs during focused mental tasks [9,23].

A simple LR classifier showed good classification accuracy and AUC, even with 25% of the channels, confirming the simple geometric RMS data pre-processing methodology. Alpha and low beta rhythms gave highest classifier accuracies rather than the dominant delta band, supporting its non-task inhibition role. The H-F class label had the worst classifier performance, while H-W showed the best, similar to previous work using the same data and an LDA classifier [4]. LDA inter-session accuracy was 64.2%±8.3% using all features and alpha band data (8-12Hz), compared to 71.5±13.1% for this LR classifier using 8.5-15.5Hz frequency band. LDA intra-session accuracies were ~79-82%±6.25% whereas the LR accuracy was 77.8±10.2%. Hence, LR achieved similar accuracy to LDA but had more variable performance. LDA with Common Spatial Pattern (CSP) feature selection showed 72% inter-session accuracy with 75 channels [4], while LR had 69.8% accuracy with 48 channels. LDA classifier performance peaked using 15 channels for MI tasks, which was not observed with LR. This might be due to unstable performance of an LDA classifier when trained with <300 features [11]. LDA AUC was sustained with less channels, while accuracy decreased [11], similar to observations with the LR classifier in this study.

IV. CONCLUSIONS

This study suggests that alpha and/or low beta SMR could be used for real-time MI based MEG-BCI using a simple LR classifier and a simple geometric RMS data pre-processing methodology.

A trained classifier's response (i.e. accuracy, AUC) could be tested using real time neuroimaging data with a variable time (sliding window of 0.1 to 0.5 secs) and different sensor numbers (50 to 204 channels) to optimise the LR classifier prediction speed (≤0.2 secs) with prediction performance. An optimal configuration could then be re-tested and deployed.

REFERENCES

[1] C. Bishop, Pattern Recognition and Machine Learning. Springer Science & Business Media, LLC, 2006.

[2] S. Aggarwal, N. Chugh, "Signal processing techniques for motor imagery brain computer interface: A review", vol. 1-2, pp 1-12, 2019.

[3] S. Baillet, "Magnetoencephalography for brain electrophysiology and imaging", Nature Neuroscience, vol. 20, no. 3, pp. 327-339, 2017.

[4] S. Roy, D. Rathee, A. Chowdhury, K. McCreadie and G. Prasad, "Assessing impact of channel selection on decoding of motor and cognitive imagery from MEG data", Journal of Neural Engineering, vol. 17, no. 5, p. 056037, 2020.

[5] Prasad, G. (2018). Brain– machine interfaces. In T. Prescott, N. Lepora, & P. Verschure (Eds.), Living machines: A handbook of research in biomimetics and biohybrid systems.

[6] L. Andersen, "Group Analysis in MNE-Python of Evoked Responses from a Tactile Stimulation Paradigm: A Pipeline for Reproducibility", Frontiers in Neuroscience, vol. 12, pp 1-18, 2018.

[7] C.Zarief, W.Hussein, #Decoding the Human Brain Activity and Predicting the Visual Stimuli from Magnetoencephalography (MEG Recordings", IMIP'19, April 19-22, 2019

[8] M. Jas, "A Reproducible MEG/EEG Group Study With the MNE Software: Recommendations, Quality Assessments, and Good Practices", Frontiers in Neuroscience, vol. 12, pp 1-30, 2018.

[9] J. Wolpaw, N. Birbaumer, D. McFarland, G. Pfurtscheller and T. Vaughan, "Brain-computer interfaces for communication and control", Clinical Neurophysiology, vol. 113, pp. 767-791, 2002.

[10] H.Halme, "Comparing Features for Classification of MEG Responses to Motor Imagery", PlosOne, vol 11, no.12, pp 1-21, 2016

[11] M. Besserve, K. Jerbi, F. Laurent, S. Baillet, J.Martinerie, L. Garnero, "Classification methods for ongoing EEG and MEG signals", Biological Research, vol. 40, no. 4, pp 415-437, 2007.

[12] S. Foldes, Magnetoencephalography. Intech, 2011, pp. 211-234.

[13] N. Gursel Ozmen, L. Gumusel and Y. Yang, "A Biologically Inspired Approach to Frequency Domain Feature Extraction for EEG Classification", Computational and Mathematical Methods in Medicine, vol. 2018, pp. 1-10, 2018.

[14] I. Xygonakis, A. Athanasiou, N. Pandria, D. Kugiumtzis and P. Bamidis, "Decoding Motor Imagery through Common Spatial Pattern Filters at the EEG Source Space", Computational Intelligence and Neuroscience, vol. 2018, pp. 1-10, 2018.

[15] Y. Wang, S. Gao and X. Gao, in Proceeding of the 2005 IEEE, Shanghai, China, pp. 5392-5395, 2005.

[16] G. Prasad, P. Herman, D. Coyle, S. McDonough, J. Crosbie, "Applying brain-computer interface to support motor imagery practice in people with stroke for upper limb recovery: a feasibility study", Journal of NeuroEngineering and Rehabilitation, vol. 7, no. 1, 2010.

[17] M. Murray, D. Brunet,C. Michel, "Topographic ERP Analyses: Step-by-Step Review", Brain Topography, vol.20, no.4, pp.249-264, 2008.

[18] M. Fard, J. Yao, K. Kato and J. Davy, "The geometric mean is a superior frequency response averaging method for human body vibration", Ergonomics, pp. 1-11, 2020.

[19] T. Harmony, "Functional significance of delta oscillations in cognitive processing", Frontiers in Integrative Neuroscience, vol. 7, 2013.

[20] D. Mwiti, "Feature Ranking with Recursive Feature Elimination in Scikit-Learn", KDnuggets, 2021. [Online]. Available: https://www.kdnuggets.com/2020/10/feature-ranking-recursive-feature-elimination-scikit-learn.html. [Accessed: 03- Jan- 2021.

[21] "Permutation Importance", Kaggle.com, 2021. [Online]. Available: https://www.kaggle.com/dansbecker/permutation-importance. [Accessed: 03- Jan- 2021].

[22] G. Pfurtscheller and F. Lopes da Silva, "Event-related EEG/MEG synchronization and desynchronization: basic principles", Clinical Neurophysiology, vol. 110, no. 11, pp. 1842-1857, 1999.

[23] W. Klimesch, "Alpha-band oscillations, attention, and controlled access to stored information", Trends in Cognitive Sciences, vol. 16, no. 12, pp. 606-617, 2012.

[24] J.Mellinger, G.Schalk, "An MEG-based Brain-Computer Interface (BCI), Neuroimage, vol 36, no. 3, pp581–593, 2007

[25] D. Rathee, H. Raza, S. Roy, G. Prasad, "A magnetoencephalography dataset for motor and cognitive imagery-based brain-computer interface," Scientific Data, vol. 8, no. 1, p. 120, 12 2021.

[26] S. Roy, S. Dora, K. McCreadie, and G. Prasad, "Mieeg-gan: generating artificial motor imagery electroencephalography signals," in 2020 IJCNN, IEEE, 2020, pp. 1–8.

[27] S. Roy, A. Chowdhury, K. McCreadie, and G. Prasad, "Deep learning based inter-subject continuous decoding of motor imagery for practical brain-computer interfaces," Frontiers in Neuroscience, vol. 14, 2020.

[28] S. Roy, K. McCreadie, and G. Prasad, "Can a single model deep learning approach enhance classification accuracy of an eeg-based brain-computer interface?" in 2019 IEEE International Conference on Systems, Man and Cybernetics (SMC). IEEE, 2019, pp. 1317–1321.

[29] S. Roy, D. Rathee, K. McCreadie, and G. Prasad, "Channel selection improves meg-based brain-computer interface," in 2019 9th International IEEE/EMBS Conference on Neural Engineering (NER). IEEE, 2019, pp. 295–298.